

COLLECTIVE EFFECTS AND IMPEDANCE UPDATE FOR THE DIAMOND-II STORAGE RING

R. Fielder*, N. Blaskovic Kraljevic, D. Rabusov,
Diamond Light Source, Oxfordshire, United Kingdom

Abstract

Impedance and collective effects are significant concerns for the design of modern accelerators. During development of the Diamond-II storage ring, effort was initially focussed on design for the arcs containing the majority of magnets, and geometric impedance was focussed on single bunch effects. We now present updates to the Diamond-II impedance database and the impact on collective effects including additional detail in straights, including injection, insertion devices and RF elements, as well as inclusion of long-range impedance for more elements for multibunch dynamics.

INTRODUCTION

Diamond-II [1] is the upcoming upgrade to the Diamond synchrotron light source. Collective effects are a major consideration for modern accelerators, given the combination of lower beam emittance with generally smaller diameter beam pipes. Ensuring instabilities will not interfere with operations by minimising beam impedance during the design stage is necessary. Diamond-II will have sixfold symmetry, with an alternating series of 48 straights and arcs. Initial design work focussed mainly on the arcs, containing the majority of magnets and responsible for many of the engineering and vacuum constraints. As this work has been completed and orders have been placed with manufacturers, design effort has progressed to the remaining components, including injection elements, insertion devices (IDs), and radio frequency (RF) systems. In this paper we present an update to the Diamond-II storage ring (SR) impedance, highlighting significant changes to both geometric and resistive wall impedance since this was last reported in 2024 [2].

RESISTIVE WALL IMPEDANCE

Resistive wall (RW) impedance for Diamond-II is calculated from an impedance database [3] containing the apertures (horizontal and vertical) and materials for the whole SR. The impedance of each component is then calculated analytically using the ImpedanceWake2D [4] code. This is split into two parts for each component, with one part containing low frequency in the longitudinal plane, while the second part goes to higher frequencies with a larger step size, as described in [2]. The total impedance is summed, including weighting with beta function in the transverse, and tracking performed in Elegant [5]. In order to simplify engineering design and manufacture, all narrow-gap vessels for out-of-vacuum IDs will now use a NEG-coated copper chamber with the same 20×8 mm full gap elliptical pro-

file in all locations. While the increased conductivity of copper compared to aluminium should reduce impedance, reducing the vertical aperture in some straights to 8 mm will largely offset this. The only exception to this is in the I06 straight, which will use a stainless steel chamber with the same dimensions to allow fast polarity switching of an electromagnetic/permanent magnet hybrid undulator (EMPHU). It has been determined that Diamond-II requires a dedicated beam abort system [6] which will use a series of fast kicker magnets to kick the stored beam into a beam dump. Again to ease design and manufacturing, these will use identical titanium-coated ceramic vessels to the injection kickers. Additional ceramic vessels have been included in the database for a pair of diagnostics pinger magnets, however, a final decision on whether these additional vessels are required has yet to be made. This results in a significant increase in the total length of ceramic vessels and a corresponding increase in impedance. The total lengths of different materials used is shown in Table 1, although apertures will vary within materials.

Table 1: Summary Of Resistive Wall Parameters In Diamond-II. Multi-Layer Materials Show Values For The Coating Followed By The Underlying Bulk Material

Material	Conductivity [S/m]	Length [m]
Copper	5.96×10^7	48.9
NEG-coated Cu	$1.00 \times 10^5, 5.96 \times 10^7$	443.4
Ti-coated alumina	$2.38 \times 10^6, 0.00$	5.0
Stainless steel	1.35×10^6	58.7
NEG-coated steel	$1.00 \times 10^5, 1.35 \times 10^6$	4.5
Total	–	560.56

Figure 1 shows the long-range resistive wall impedance of the updated impedance model.

GEOMETRIC IMPEDANCE

Geometric impedance is calculated using the wakefield solver in CST Studio [7]. Short range wakes are calculated using a $\sigma = 0.5$ mm drive bunch length and 300 mm wake length, which have been determined to give convergence in Elegant while allowing reasonable simulation times. Some larger models, such as dipole vessels, instead use a $\sigma = 1.0$ mm drive bunch to reduce the number of mesh cells required. Dipolar wakes have been calculated for all components, while quadrupolar and monopolar wakes are calculated for components with significant asymmetry, and are being added for all other components as computing resources allow. Short range impedance is calculated using all perfect conductor (PEC) material, except in some cases containing

* richard.fielder@diamond.ac.uk

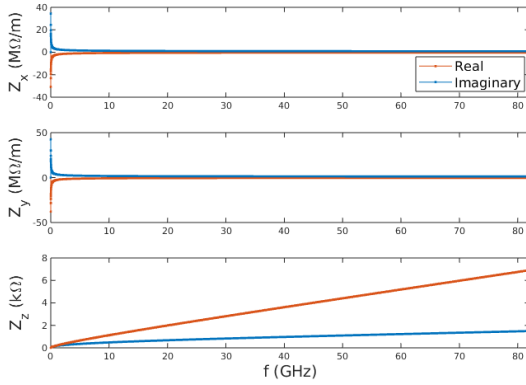


Figure 1: Resistive wall impedance for the Diamond-II SR. Horizontal (top), vertical (middle) and longitudinal (bottom).

significant non-metallic materials such as ceramics. The total short range geometric wake is shown in Fig. 2. Long range geometric impedance is calculated using a $\sigma = 8$ mm drive bunch length where possible, although large models may require a longer bunch due to computational constraints, and a 250 m wake length. Long range wakes are calculated using real material properties to introduce damping to the wake [2]. Long range wakes have initially been calculated for components expected to show large resonances, and have been added for other components as computing time allows.

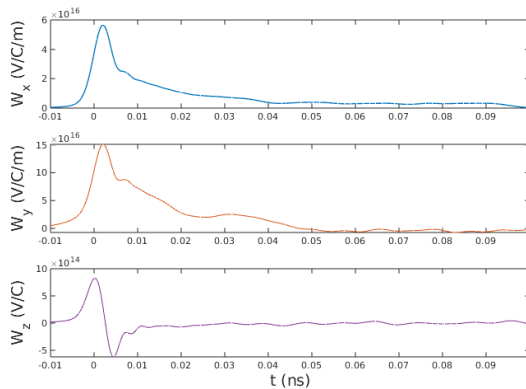


Figure 2: Total geometric wake function for Diamond-II. Horizontal (top), vertical (middle) and longitudinal (bottom).

Collimators

The horizontal and vertical collimators for Diamond-II both use the same design, shown in Fig. 3, rotated by 90 degrees relative to each other, with the blades at a nominal 7 mm gap for the horizontal and 3 mm gap for the vertical. The design has been updated after discussions with the manufacturer, resulting in shorter, steeper fixed tapers. Long range wakefields were previously not included for the vertical collimator while the design progressed, and these make one of the most significant impacts to the long-range

impedance due to the closeness of the blades to the electron beam.

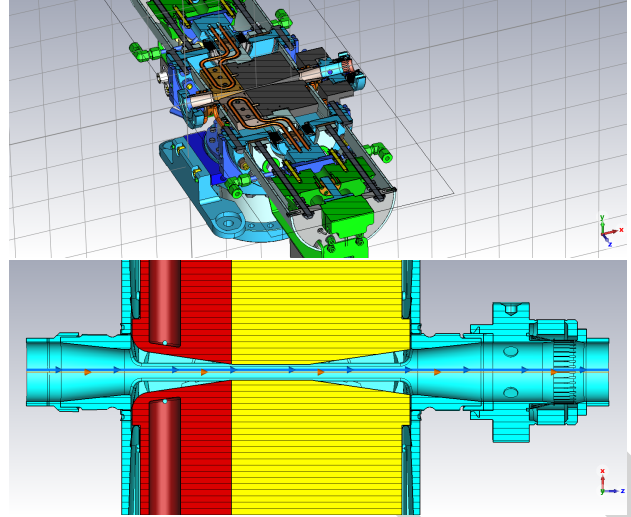


Figure 3: Full engineering model (top) and cutaway view of simplified simulation geometry for the horizontal collimator, where blue is stainless steel, yellow is tungsten and red is copper, with the beam and integration paths indicated by the blue and orange arrows respectively.

RF

The RF cavities take up five mid-straight in Diamond-II. Main RF has eight normal-conducting cavities split across four identical straights (K05, K09, K10, K15), while a superconducting higher harmonic cavity (HHC) is in K17, close to existing cryogenic systems for the current superconducting RF cavities. The RF cavities themselves are included in tracking simulations using modal analysis from eigenmode simulations, since their large resonant structures are difficult to simulate in the time domain. Impedance for the remainder of the straights are simulated normally using the wakefield solver. The geometric impedance for the K17 straight, excluding the cavity itself, is included in the impedance database. Design work is still in progress for the main RF straights, so the impedance database currently only includes the resistive wall impedance for these. The engineering model for the main RF straights is shown in Fig. 4.

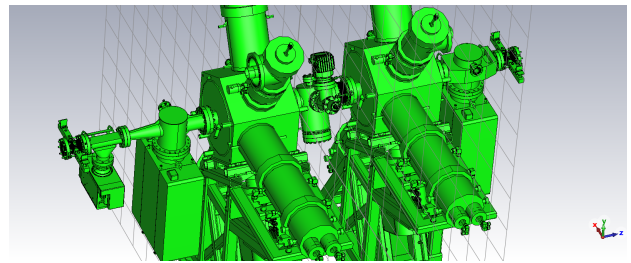


Figure 4: Engineering model for the main RF straights.

Injection

Injection systems for Diamond-II are split across two straights. The I01 long straight contains four pulsed kicker

magnets, an electromagnetic thin septum magnet, and a combined permanent magnet/electromagnetic main septum magnet. Design work is still in progress for the main septum, so this is not yet included in the database. The design of the K01 mid-straight containing the stripline kickers for kick-and-cancel injection [8] is largely settled, having had only minor updates to photon absorbers and pumping sections.

IDs

Design for ID straights is a work in progress. Both in- and out-of-vacuum IDs are included as part of the resistive wall impedance, but details of tapers and transitions at the ends of straights are mostly not yet included. Since IDs are large, simulating an entire straight is computationally expensive. A generic model of an in-vacuum ID has been created to test the feasibility of simulating the full straight. This has shown that it is possible to simulate a relatively simple model of an ID vessel in a 2.4 m long straight with 160 mm radius. However, work remains to test how variations in dimensions or addition of more detail affect the results, to determine if this generic model would be valid for inclusion in the impedance database.

Beam Dumps

The beam abort system [6] will take up two identical mid-straights, K23 and K24. The ceramic kicker vessels are already included in the resistive wall impedance, as noted above. Detailed design work on the straights is ongoing, so there is as yet no geometric impedance. These straights will contain steep transition tapers and come close to the electron beam path, as shown in Fig. 5, so impedance is an important consideration for the design.

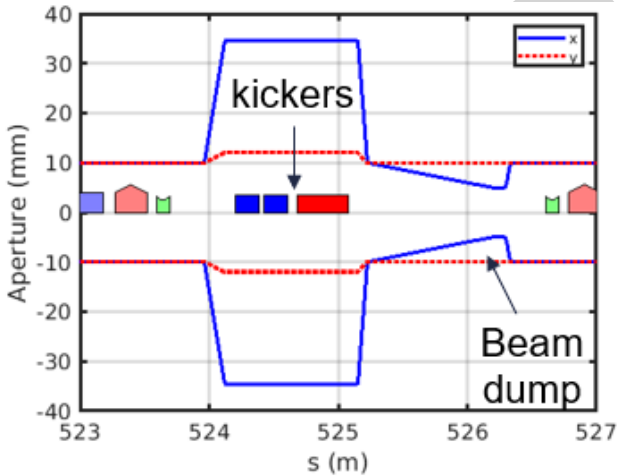


Figure 5: Approximate apertures through K23 straight.

RESULTS

Coupled-bunch instability growth rates including all resistive and geometric impedance are shown in Fig. 6. In the horizontal, the largest growth rates are due to the injection striplines, which have the most impact around modes 870-910. The large peaks in the vertical around modes 300

and 600 come from the vertical collimators. With IDs open these are the most unstable modes, while with IDs closed the resistive wall still dominates. Previous tracking simulations indicate that operating at chromaticity above +2 in both planes and adjusting the fill pattern, in combination with the HHC and/or multibunch feedback systems is sufficient for stability at 300 mA.

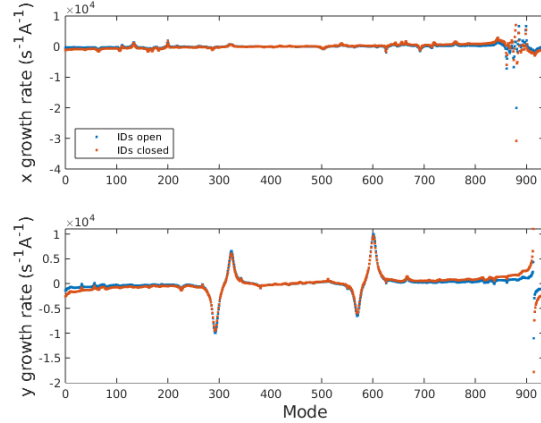


Figure 6: Coupled-bunch instability growth rates at zero chromaticity, uniform fill, including all RW and geometric impedance, comparing IDs open and closed. Horizontal (top) and vertical (bottom).

CONCLUSION

The design of Diamond-II has progressed significantly, with most vessels in the arcs finalised and many components already contracted for manufacture. The impedance model and corresponding particle dynamics and instability thresholds have been updated to match. Focus is now on the remaining components, especially the injection and ID straights.

REFERENCES

- [1] Diamond Light Source, *Diamond-II Technical Design Report*. <https://www.diamond.ac.uk/Diamond-II/Technology.html>, accessed 27 Apr. 2026.
- [2] R. Fielder, D. Rabusov, and S. Wang, "Updates to the impedance database for the Diamond-II storage ring", in *Proc. IPAC'24*, Nashville, TN, USA, May 2024, pp. 3112–3115. doi:10.18429/JACoW-IPAC2024-THPC50
- [3] R. T. Fielder and T. Olsson, "Construction of an impedance model for Diamond-II", in *Proc. IPAC'21*, Campinas, Brazil, May 2021, pp. 455–458. doi:10.18429/JACoW-IPAC2021-MOPAB127
- [4] ImpedanceWake2D. <https://twiki.cern.ch/twiki/bin/view/ABPComputing/ImpedanceWake2D>, accessed 27 Apr. 2026.
- [5] M. Borland, "elegant: A flexible SDDS-compliant code for accelerator simulation", Advanced Photon Source, Lemont, IL, USA, Rep. LS-287, Sep. 2000. doi:10.2172/761286
- [6] H. Ghasem, I. P. S. Martin, W. Shields, and A. Potter, "A beam abort system for the Diamond-II storage ring", presented at

IPAC'26, Deauville, France, May 2026, paper WEP6138, this conference.

[7] CST Studio Suite. <https://www.3ds.com/products/simulia/cst-studio-suite>, accessed 27 Apr. 2026.

[8] A. Lueangaramwong *et al.*, “Kick-and-cancel injection scheme for the Diamond-II storage ring”, *Phys. Rev. Accel. Beams*,

vol. 28, no. 6, p. 060701, 2025.

[doi:10.1103/PhysRevAccelBeams.28.060701](https://doi.org/10.1103/PhysRevAccelBeams.28.060701)

[9] D. Rabusov, R. Fielder, and S. Wang, “Analysis of single-bunch instabilities for Diamond-II”, in *Proc. IPAC'23*, Venice, Italy, May 2023, pp. 3550–3553.

[doi:10.18429/JACoW-IPAC2023-WEPL184](https://doi.org/10.18429/JACoW-IPAC2023-WEPL184)

PREPRINT